

Introducing ADAPTSMOOTH*, a new code for the adaptive smoothing of astronomical images

Stefano Zibetti[†]

Max-Planck-Institut für Astronomie, Königstuhl 17, D-69117 Heidelberg, Germany

Abstract

We introduce and publicly release a new standalone code, ADAPTSMOOTH, which serves to smooth astronomical images in an adaptive fashion, in order to enhance the signal-to-noise ratio (S/N). The adaptive smoothing scheme allows to take full advantage of the spatially resolved photometric information contained in an image in that at any location the minimal smoothing is applied to reach the requested S/N. Support is given to match more images on the same smoothing length, such that proper estimates of local colours can be done, with a big potential impact on multi-wavelength studies of extended sources (galaxies, nebulae). Different modes to estimate local S/N are provided. In addition to classical arithmetic-mean averaging mode, the code can operate in median averaging mode, resulting in a significant enhancement of the final image quality and very accurate flux conservation. To this goal also other code options are implemented and discussed in this paper. Finally, we analyze in great detail the effect of the adaptive smoothing on galaxy photometry, in particular to check for conservation of surface brightness (SB) and aperture-integrated fluxes: deviations in SB with respect to the original image can be limited to < 0.01 mag, with flux difference in apertures of less than 0.001 mag. With respect to already existing adaptive smoothing codes, mainly developed by the X-ray community, ADAPTSMOOTH uniquely provides the median averaging mode and a greater flexibility

to adapt to different noise regimes and degrees of image contrast, which can occur especially in optical and near-IR imaging.

Keywords: techniques: image processing, photometric.

1 Introduction

Extended astronomical sources, like galaxies and nebulae, are characterized by a huge dynamical range of surface brightness (SB) throughout their extent. This range spans several orders of magnitude and can be captured by current astronomical imaging devices at optical and near-IR wavelengths. However, as a consequence the signal-to-noise ratio (S/N) of the information contained in the image varies wildly depending on the (surface) brightness at any given position. Therefore the problem arises how to extract the information by optimally balancing the S/N of the flux measurement and the effective spatial resolution.

Imaging devices are typically operated in background noise limited conditions, i.e. the main source of noise comes from the background rather than from the Poisson photon noise of the source itself, which becomes dominant only at very high S/N levels. While the background noise puts a well defined lower limit to the brightness of very localized/point-like sources that can be detected at a given S/N, when imaging diffuse objects the detection limit and the S/N at which a given surface brightness is measured can be improved by combining the flux measured in increasingly more pixels. Two approaches are available to do this: binning and filtering (or smoothing). In the first case, a number N of pixels that share a

*Available at <http://www.wiki-site.com/index.php/ADAPTSMOOTH>

[†]Current address: DARK Cosmology Centre, Niels Bohr Institute, University of Copenhagen, Juliane Maries Vej 30, 2100 Copenhagen Ø, Denmark, zibetti@dark-cosmology.dk

similar intensity level and/or match given spatial constraints are averaged, resulting in an improvement in S/N of \sqrt{N} , in the ideal case of uniform uncorrelated noise. Examples of the binning approach are azimuthally averaged profiles of the surface brightness of galaxies along elliptical isophotes (e.g. the algorithm of Busko 1996; Jedrzejewski 1987, as implemented in the IRAF task *ellipse*) and the tessellation algorithms that are extensively utilized in the analysis of integral field spectroscopic observations (for an implementation see Cappellari & Copin 2003). As a result of binning, the number of resolution elements is decreased (hence the spatial resolution is worsened or even the dimensionality is lowered) and all the available information in the image is compressed at a higher S/N level. The filtering (or smoothing) approach consists in cutting the highest spatial frequencies that contribute most of the noise. The result of filtering is a smoothed image, where the intensity of each pixel is replaced by a weighted average of the neighbouring pixels, over an extent and with a weighting scheme that depend on the particular kernel adopted. Popular choices of kernels are 2D gaussians and top-hat functions (resulting in the so-called ‘boxcar’ smoothing). As with the binning, also in the filtering approach the S/N is increased by a factor of the order of \sqrt{N} (where N is the number of pixels in the kernel). Although the number of spatial elements (pixels) is preserved, the information in the smoothed image is correlated and spatial resolution is lost, proportionally to the kernel size. In fact, by cutting the highest spatial frequencies not only the noise but also the sharpest features of the image are thrown away.

Both approaches have of course their own pros and cons. Filtering/smoothing, in general, offers the best 2D rendition of the information, although it is often non-optimal in terms of compromise between spatial resolution and S/N enhancement, which, reversely, is a point of strength of the tessellation algorithms. In the regions of high surface brightness (SB) the S/N is high, such that no or minimal smoothing is requested, while smoothing with increasingly larger kernels is required to enhance the S/N of lower and lower SB regions to acceptable levels. The optimal solution is to apply to the image a smoothing with

variable kernel size, which matches the local S/N: this is what is called *adaptive smoothing*.

The X-ray community, pushed by the necessity to deal with diffuse sources in very low S/N regimes, has produced a number of codes to implement this basic concept. A (possibly incomplete) list includes: FADAPT (distributed as part of the package FTOOLS, Blackburn 1995); Huang & Sarazin (1996); ASMOOTH (included in the Chandra data reduction package CIAO, also known as CSMOOTH in the IDL implementation, Ebeling et al. 2006); Sanders (2006); ASMOOTH in the XMM-Newton Science Analysis System.

The new, standalone, adaptive smoothing code ADAPTSMOOTH presented in this paper has been developed with in mind mainly typical optical and near-IR imaging (although its application at other wavelengths is well supported too) and allows to easily handle different S/N regimes, even in cases where very limited information about the noise properties of the images are available, as detailed in Sec. 2.2. We introduce *median* adaptive smoothing in addition to the *mean* adaptive smoothing, which is the only method implemented in the other codes mentioned above. The improvement deriving from using the median as average estimate is especially notable in presence of strong intensity gradients (e.g. bright point-like sources overlaid on an area low surface brightness) and is thoroughly illustrated in Sec. 3. We also provide different methods to prevent cross-talking between pixels at different S/N levels, which can be switched on or off by the user (see Sec. 2.3) as opposed to the rigid implementation (e.g. A/CSMOOTH, Ebeling et al. 2006) or lack of them in other codes. Similarly to A/CSMOOTH in CIAO and ASMOOTH in the XMM package, ADAPTSMOOTH outputs maps of the smoothing length at each location (“smoothing masks”) and allows to use them as input for smoothing other images: this feature allows matching smoothing scales across different images and is therefore essential to produce, e.g., color maps (see Sec. 2.4).

ADAPTSMOOTH is made publicly available via this URL <http://www.wiki-site.com/index.php/ADAPTSMOOTH> or on request to the author. In the following sections

we describe the concept of the algorithm and the actual code implementation with the available options. We show a couple of examples on astronomical images. Finally we analyze in detail the reliability of the code output in terms of conservation of flux and surface brightness in order to perform accurate surface photometry (specifically of galaxies) in different conditions.

2 Adaptive smoothing with ADAPTSMOOTH

2.1 Concept

We design the ADAPTSMOOTH code to smooth an input image with a variable-size kernel in order to provide the measure of the local surface brightness with S/N equal to (or larger than) a minimum user-provided value at any location. The size of the kernel is determined locally (at each pixel) and iteratively as the minimum size that allows to reach the requested S/N. In this sense, the ADAPTSMOOTH algorithm is optimized to retain the maximum of spatial resolution that is compatible with the requested S/N. As mentioned above, this basic concept is common to most adaptive smoothing codes. The main differences among codes reside in the way S/N is defined and computed and in the way smoothing is actually performed (type of kernel, weighting, FFT vs window sliding convolution, etc.).

Here is a description of basic steps of the ADAPTSMOOTH algorithm. We assume that a background-subtracted image and the requested minimum S/N are input. At each pixel i an estimate of the local noise $n_{i,1}$ is performed (see Section 2.2). The pixel brightness $f_{i,1}$ is compared with the noise and if $f_{i,1}/n_{i,1} > S/N$ then the current pixel value is retained and the procedure goes to the next pixel, else smoothing is requested. In this case, a new estimate of the local surface brightness $f_{i,2}$ is computed as the average in a circle of radius 1 pixel centered on the pixel i . The corresponding uncertainty $n_{i,2}$ is computed and a new S/N check is performed: if $f_{i,2}/n_{i,2} > S/N$ then the current SB estimate $f_{i,2}$ is assigned to the pixel, else further smoothing is re-

quired. The procedure is repeated increasing the radius of the circle by 1 pixel each time and is iterated until the S/N condition is satisfied or the maximum radius for the circle is reached. It must be noted that in the ideal case of uncorrelated noise and no systematic background offsets, the S/N condition is met in any case after a large enough number of iterations, as $f_{i,l}/n_{i,l} \propto l$ (in the following we call l ‘smoothing level’). In reality, beyond a smoothing level of a few tens correlated noise and systematics prevent the smoothing procedure to produce any real S/N enhancement.

We note that ADAPTSMOOTH, contrary to other codes, just implements top-hat kernels, such that no (i.e. uniform) weighting is applied when averaging. We do not feel this is a relevant limitation since weighting more on the central pixels when the distribution is dominated by noise is not expected to change the results significantly. On the other hand, the speed of the algorithm can substantially benefit from avoiding weights in computing average quantities.

In ADAPTSMOOTH the user can choose between median and arithmetic mean as the average that is used to estimate the local SB inside the kernel radius. This feature is unique to the present code. As we demonstrate in Sec. 3, the two methods perform very similarly in absence of strong peaks in the SB distributions, but using the median results in a much better behaved response in the vicinity of strong discontinuities. However, one notable case where mean averaging must be used in place of median averaging is when the photon statistics is extremely poor, at the limit of binarity. This occurs for example in UV or X-ray images where most of the pixels have either one or zero counts: in this case one must use mean averaging in order to obtain a fair representation of the surface brightness field, while median averaging would produce just an almost random binary map (see Salim & Rich 2010, for a successful application of ADAPTSMOOTH with mean averaging in this regime).

In the next two sub-sections we describe the features of the code that allow the user an optimal computation of the noise and to keep the generation of artifacts under control. In Sec. 3 the effect of these

features on images and surface photometry of galaxies will be shown and tested in detail.

2.2 Noise estimates

A realistic estimate of the local noise is central to properly determine the kernel size for smoothing. ADAPTSMOOTH offers three possible methods to estimate noise.

- i)* Poisson+background noise – The following equation for the noise σ is assumed:

$$\sigma^2 = \sigma_{\text{bkg}}^2 + f/G \quad (1)$$

where f is the brightness of the pixel in counts (analog-digital units, ADU), σ_{bkg} is the background r.m.s. noise in ADU (which includes the contributions from the sky background, read-out noise and dark current) and G is the gain, i.e. the number of photo-electrons per ADU. The last two numbers must be measured/known beforehand and input to the code, which assumes they are constant throughout the image. In the hypothesis of uncorrelated noise, when the smoothing circular aperture is considered, the background component of the noise σ_{bkg} is simply assumed to rescale as \sqrt{N} , N being the number of pixels in the aperture. The Poisson+background noise is the recommended mode in all cases, unless strong variations of σ_{bkg} or G are present in the image.

- ii)* Background-dominated noise – In most astronomical image applications, in the regime of SB where smoothing becomes relevant, one can safely assume background dominated noise, which corresponds to Eq. 1 with infinite gain or $f/G = 0$. This is done in background-dominated noise mode, for which only σ_{bkg} is to be input. This can be particularly useful when the effective gain is not easily accessible or computable (e.g. near-IR stacks).
- iii)* Direct local noise estimate – ADAPTSMOOTH can compute the noise locally, without any prior knowledge of the image properties, as the r.m.s.

counts in a circular aperture centered on the current pixel. A radius 2 pixels larger than the current smoothing level is adopted in this case to ensure sufficient statistics especially at the lowest smoothing levels. This mode offers a viable solution for images in which background dominated noise cannot be assumed yet the photon statistics is ill-determined, like, for instance, digitized photographic plates or digital images with unknown and/or significant gain or background noise variations across the field. However, modes *i)* and *ii)* should be preferred whenever possible, in order to avoid the artifacts that can arise from adopting direct local noise calculation. Especially in the proximity of sharp features the local r.m.s. is dominated by SB fluctuations due to the real objects, which leads to severe noise overestimation and hence oversmoothing.

To our knowledge, ADAPTSMOOTH is the only code offering these three choices of noise computation¹, which cover all possible user's requests in typical optical/near-IR imaging.

2.3 Cross-talking between smoothing levels

A potential problem of the adaptive smoothing scheme is that the estimated SB of pixels in high smoothing levels (i.e. low original S/N) is affected by neighbouring pixels at lower smoothing levels, which have higher S/N and brightness: we call this effect ‘cross-talking’ between smoothing levels. As we show in Sec. 3, the cross-talking can artificially broaden sharp bright features (such as stars), especially when the arithmetic mean is chosen as average estimator instead of the median. Moreover, this effect may result in not conserving the mean SB of the image, because of the asymmetry of the cross-talking: bright pixels require less smoothing and therefore are only marginally affected by neighbouring lower-SB pixels, while lower-SB pixels may be made significantly

¹FADAPT just considers pure Poisson noise, CIAO CSMOOTH supports background dominated and Poisson noise, and XMM ASMOOTH support only Poisson mode and user pre-computed variance maps.

brighter by smoothing over larger areas that might include bright pixels.

To limit the cross-talking we introduce the option of excluding pixels with lower smoothing levels from the computation of the average smoothed SB. Specifically, the ‘level cut’ parameter ‘c’ can be specified to exclude either smoothing level 1 from the other levels ($c = 1$), or to make a relative cut to exclude all levels but those higher than the current $-n$ (any $c < 0$, $c = -n$). This option is switched off by default.

We note that CIAO CSMOOTH implements a similar solution to limit cross-talking, which essentially corresponds to setting $c = -1$ in ADAPTSMOOTH. However, contrary to ADAPTSMOOTH which allows the user full flexibility, this option is hard-coded in CSMOOTH and no choice is given to the user if and to which degree to use it.

2.4 Matching images in input-mask mode

By default ADAPTSMOOTH determines the smoothing level of each pixel by a direct analysis of the image, as explained above, and outputs the smoothed image and an image containing the smoothing level of each pixel, which we dub ‘smoothing mask’. This is useful in first place for checking purposes, to understand how the image has been elaborated. Many astronomical applications make use of multi-band imaging to derive spatially resolved physical information, for instance colour maps that serve to determine the stellar mass distribution or the spatial variation of the SED in a galaxy, flux-ratios maps in narrow-bands to extract extinction maps in star-forming regions, etc. For all this kind of applications it is crucial that the spatial resolution of the images in different bands are perfectly matched, so that the flux measurements are consistent. ADAPTSMOOTH-ed images have varying effective resolution across the field depending on the S/N of the pixels, which in turn depend on the observed band and the observing conditions. In order to obtain consistent flux measurements in two or more bands it is necessary to smooth the corresponding images in the same way. To do this we allow the user to force ADAPTSMOOTH to use pre-determined smoothing levels.

The standard procedure to match a number of ADAPTSMOOTH-ed images (which we assume to be already accurately registered to the same plate scale) is as follows. First, one has to run ADAPTSMOOTH on the individual images in the standard mode to obtain the requested S/N (which can be different in each image); for each image, the smoothing mask is output, which contains the *minimum* smoothing level required at each pixel to obtain the requested S/N. The smoothing masks have to be combined to retain the maximum value at each pixel. Finally, ADAPTSMOOTH needs to be run a second time on each image by giving the combined smoothing mask *as input*. In this way the requested minimum S/N is ensured at all pixels, while the same smoothing is performed in all images.

2.5 Technical notes on the code

ADAPTSMOOTH is a standalone code written in C language and works as line command with standard GNU options parsing. Graphical user interface will be provided in future releases. All image input/output is based on the standard C library CFITSIO (Pence 1999), not provided with the code.

Execution time depends critically on the chosen mode, the properties of the image and the requested S/N. In our tests with a 2.4 GHz processor typical execution times range between a few seconds up to 5-6 minutes for a $1k \times 1k$ image. Mask-input mode is always faster than the standard mode; using mean average is slightly faster than median average; local-noise takes significantly longer than Poisson or background only; with ‘level cut’ enabled the execution time is practically twice as much as in standard mode with the same set of parameters.

In order to speed up the access to the pixels in the smoothing apertures, their relative coordinate offsets with respect to the current image position are pre-computed up to the 27th smoothing level and stored in a static array. This limits the smoothing level that can be used to 27.

In local noise mode ADAPTSMOOTH approximates the r.m.s. with half of the 16th–84th percentile range, as it is more robust against outliers. For this and for median estimates a fast selection algorithm is needed.

After some testing, we opted for an implementation of the algorithm by Floyd & Rivest (1975).

It is worth noting that when the ‘level cut’ option is enabled (see Sec. 2.3) the code works in two passes, hence it is roughly twice as slow. The first pass provides a preliminary smoothing level for each pixel and the second pass computes the actual smoothed image where the level cuts are properly accounted for. Although in principle more passes might be necessary to converge to the final determination of smoothing levels, we checked that in most practical cases two passes are enough.

2.6 Enhancing imaging and photometry with ADAPTSMOOTH

The adaptive smoothing technique may have a big impact on a number of astronomical fields where spatially resolved flux information is required over a large dynamical range of surface brightness. Zibetti et al. (2009, 2010) showed how the adaptive smoothing can be applied to galaxies to map their colours and eventually derive the stellar mass density distribution and its link with local SED. Mentuch et al. (2010) successfully exploited the power of the adaptive smoothing technique to identify the regions responsible for NIR excess in the SED of star-forming galaxies. ADAPTSMOOTH has also been used by Martínez-Delgado et al. (2010) and Martínez-Delgado et al. (in preparation) to estimate optical colors and calibrate the photometry of ultra-faint diffuse streams of stars around nearby galaxies.

In Fig. 1 we illustrate the full power of the adaptive smoothing technique on a emission-line ratio map of the star-forming HII region NGC 2024 (Bik et al. 2003). $\log \frac{\text{Paschen}\beta}{\text{Brackett}\gamma}$ is computed for each pixel and shown as grey-scale in the two panels of Fig. 1. Panel *a*) (to the left) shows the line-ratio map as obtained from the original images. The pixels highlighted in red are those for which either of the two images has zero or negative intensity. The right-hand panel *b*) displays the map obtained from ADAPTSMOOTHED images with minimum S/N of 10 in both bands, obtained using median averaging and assuming background dominated noise. The smoothing in the two original pass-band images is matched as explained in

Sec. 2.4. Pixels for which the minimum S/N could not be reached are painted in red. It is immediate to see *i*) the large number of pixels for which the line ratio becomes measurable only after ADAPTSMOOTHing and *ii*) the detail which is gained in the map thanks to the increased S/N provided by ADAPTSMOOTH, which in this case guarantees errors smaller than 15 per cent on the line ratio in each individual pixel as opposed to the huge scatter obtained without adaptive smoothing. Similarly to this application, Pasquali et al. (2011) use ADAPTSMOOTH to produce deep, high-resolution maps of near-IR line emissions in the nearby dwarf star-bursting galaxy NGC 1569, which in turn are used to derive maps of dust extinction and extinction-corrected star-formation rate of unprecedented accuracy and detail.

This shows that by adaptively smoothing optical and near-IR images it is possible to produce extremely accurate, deep and high-resolution colour and line ratio maps using currently available datasets, at no extra expense in terms of telescope time. In turn this opens up the opportunity to perform spatially resolved analysis of SED and dust extinction throughout extended object such as nebulae and galaxies.

3 Testing ADAPTSMOOTH with galaxy photometry

In this section we test the performance of ADAPTSMOOTH on the image of a galaxy, using different modes and parameters. We choose NGC 5713 as imaged in *r* band in the Sloan Digital Sky Survey (SDSS, York & et al. 2000). This galaxy displays a complex enough structure so that the code can be tested in relatively extreme conditions, while the SDSS is chosen as representative of present-day sources of astronomical images.

3.1 Morphological tests

The panel *a*) of Fig. 2 shows the original SDSS *r*-band image of the galaxy. Panels *b*) and *c*) show the ADAPTSMOOTH-ed images obtained for a minimum S/N of 20, with median average, maximum

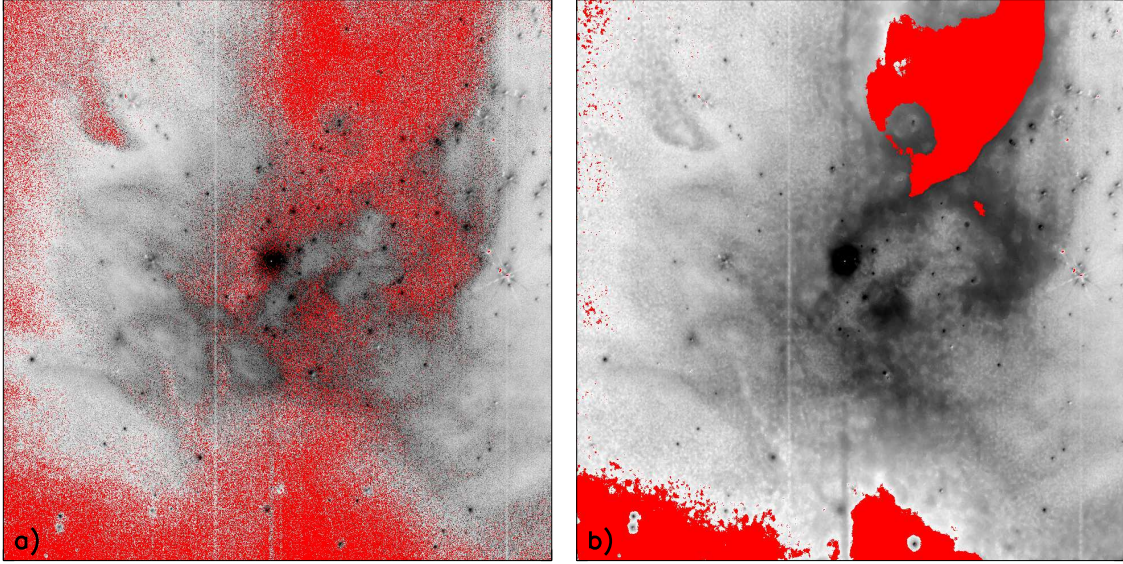


Figure 1: The map of $\log \frac{\text{Paschen}\beta}{\text{Brackett}\gamma}$ for the emission nebula NGC 2024 (from Bik et al. 2003). Panel *a*) shows the map as obtained from the original images. Panel *b*) displays the map obtained after median-average smoothing the images with ADAPTSMOOTH to a minimum S/N of 10 (background dominated noise is assumed). Red is used in panel *a*) for pixels where fluxes are zero or negative in the original images; in panel *b*) red identifies areas where the minimum S/N could not be reached. ADAPTSMOOTH retains the highest resolution in the high-SB regions, while enhancing the S/N and therefore allowing meaningful measurements at low-SB by using the minimal required smoothing.

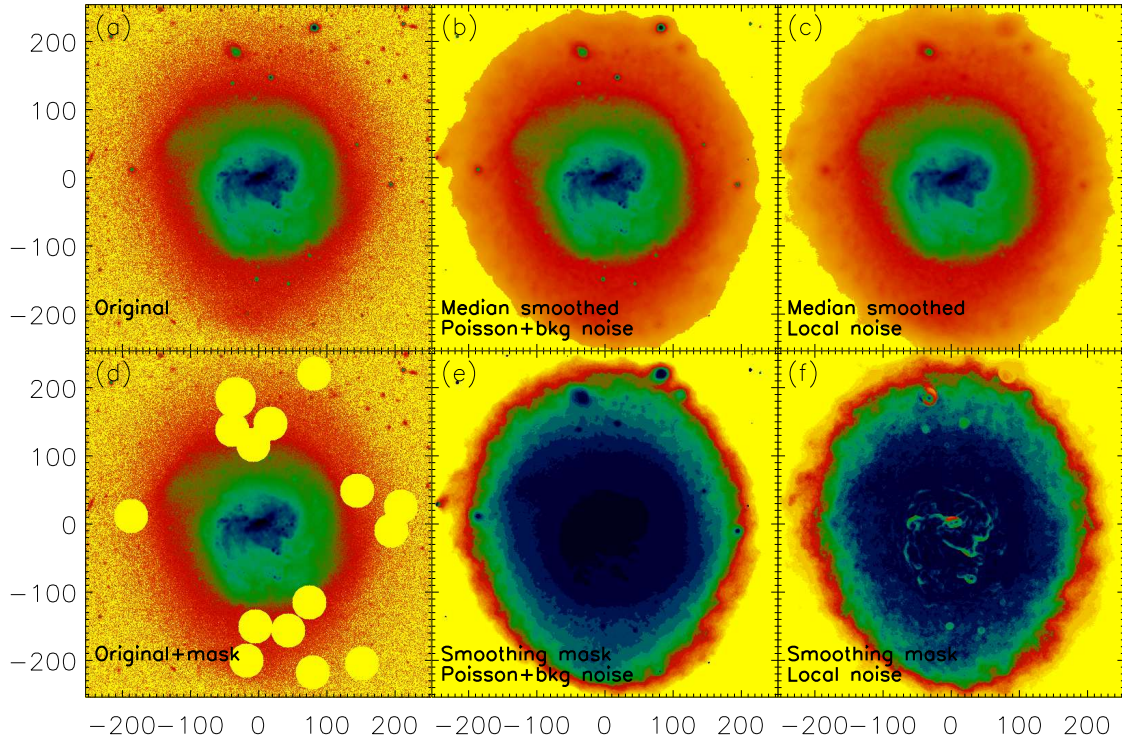


Figure 2: The galaxy NGC 5713 as our benchmark for testing ADAPTSMOOTH. Original SDSS *r*-band image (panel *a*)); ADAPTSMOOTH-ed image (median-averaging, $S/N > 20$) with Poisson+background noise estimation (panel *b*)); ADAPTSMOOTH-ed image (median-averaging, $S/N > 20$) with local noise estimation (panel *c*)); original SDSS *r*-band image with overlaid masks for problematic regions (panel *d*)); smoothing mask relative to panel *b*) (panel *e*); smoothing mask relative to panel *c*) (panel *f*). The colour scales for the images cover the entire dynamical range with a logarithmic stretch, which is kept the same in all images. For the masks, colours go linearly from dark blue (smoothing level 1) to orange/yellow (level 20).

smoothing level of 20 and no level cuts. In panel *b*) the Poisson+background noise estimate is used, whereas a purely local noise estimate from the image is adopted in panel *c*). A careful comparison of the two smoothed images shows that a number of localized sharp features that are seen in *b*) completely disappear, smoothed out, in *c*). These include stars, but also star-forming regions and bright stellar knots in the central regions of the galaxy. A comparison of the corresponding smoothing masks (panels *e*) and *f*), where the smoothing levels are coded from blue to red/yellow going from 1 to 20) highlights the fact that noise estimates based on the local r.m.s. result in grossly overestimating the smoothing radii requested in the vicinity of sharp features. While the Poisson+background noise model correctly recognizes that nowhere in the central parts of the galaxy substantial smoothing is needed to enhance the S/N, based on the local r.m.s. the code performs massive smoothing at several locations down into the nucleus. On the other hand, far from sharp structures the smoothing levels assigned with the two methods are in excellent agreement, as one can see looking at the overall structure of the smoothed images and, even better, of the smoothing masks. To summarize, the local noise mode can give substantially correct results in smooth areas, but should be avoided in presence of sharp structures.

We have also compared the Poisson+background noise mode with the pure background noise mode (not shown) and find practically no difference, with the exception of a very small number of pixels jumping from smoothing level 2 to 1 (i.e. no smoothing) when the Poisson contribution is neglected. This was expected as we know that SDSS images are in the regime of background dominated noise. In the rest of the analysis we consider only noise estimated based on the Poisson+background model.

In Fig. 3 we compare smoothed images obtained with the two different average options, median (upper row) and mean (lower row), and with different level cuts. In this figure we show only a zoomed-in region of the same galaxy NGC 5713, in order to better highlight the differences. The first panel of each row (viz. *a*) and *d*)) shows the results for no smoothing level cuts, the second panel (viz. *b*) and

e)) is obtained excluding level 1 from all other levels, and the third panel (viz. *c*) and *f*)) is the image obtained by excluding all smoothing levels up to the current one minus 2. The first thing to note in Fig. 3 is that using the mean results in broadening the SB peaks over significantly large areas, especially when the peak is in the middle of a low-SB region where substantial smoothing is applied. This is particularly evident for the source located at (80,-215), but also for other sources, most likely foreground stars. The median smoothing is more robust against this cross-talking effect because a few high-SB pixels falling inside a large smoothing aperture, where most pixels have much lower SB, negligibly affect the median value, but can substantially alter the mean. Smoothing level cuts are meant to reduce the cross-talking effect. From panels *a*), *b*) and *c*) we see that the cuts do not produce any visible effect on the broadening of bright peaks when the median is used, confirming that the median estimate already produces optimal results in this sense. On the contrary, using smoothing level cuts when the mean average is adopted can strongly reduce the broadening (panels *d*), *e*), *f*)). Excluding only the highest-SB pixels (level 1) can help only with very bright sources, such as the star at (0,-148), while a relative cut (in this case, considering only the levels higher than the current one minus 2) significantly reduces the broadening for all peaks. A second effect of using a relative cut is seen at the lowest SB, where the exclusion of higher SB levels produces lower SB in the images with cuts with respect to those without cuts. This effect can be seen comparing the yellow area, which corresponds to minimum S/N not reachable, of panels *c*) (or *f*)) and *a*) (or *d*)): applying no cuts results in a larger area with acceptable S/N.

3.2 Quantitative tests

In Figures 4 and 5 we analyze how the adaptive smoothing with different modes and parameters affects the SB distributions in pixels, on a pixel-by-pixel base and in terms of azimuthally averaged profiles and aperture photometry, respectively. The analysis performed in this section is not meant to be illustrative of typical possible applications of

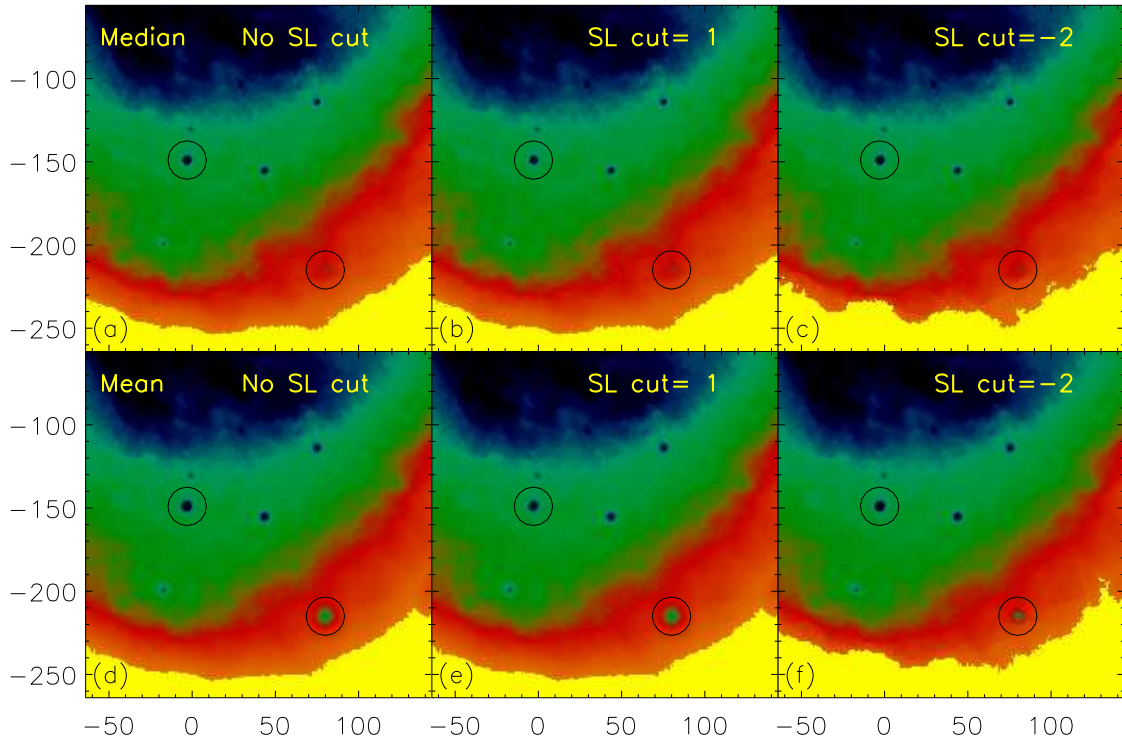


Figure 3: The effect of different smoothing modes and smoothing level cuts are illustrated in this Figure, for a zoomed-in region of NGC 5713. The *top* row (panels *a*), *b*), *c*)) show images obtained using median-averaging, while for the *bottom* row (panels *d*), *e*), *f*)) mean-averaging is adopted. In the *first* column (panels *a*), *d*)) no smoothing level cut is used; in the images of the *second* column (panels *b*), *e*)) level 1 is excluded from the computation of the other levels; the *third* column (panels *c*), *f*)) shows the results for excluding all levels up to the current -2 . Two features are highlighted (black circles) where the effects of the different smoothing modes are particularly evident.

ADAPTSMOOTH to galaxy photometry. In fact, all photometric measurements involving binning, averaging and integrating within apertures are better performed on original unsmoothed images. Here we just want to show that the output of ADAPTSMOOTH is not biased and average surface brightness and fluxes in different apertures are conserved.

In first place we bin all pixels in the image in elliptical annuli, centered on the galaxy centre and with ellipticity and position angle corresponding to the outer isophotes. Secondly, we consider two versions of the images: the full image and one where some regions are masked out (shown in panel *d*) of Fig. 2). The masked regions correspond to bright spots on top of a smoother low-SB background, where the largest differences between different methods is observed, as shown in the previous paragraph.

In the six panels of Fig. 4, we consider *for each pixel* the relative difference between the SB in the smoothed image and the original image, given by $\delta = (\Sigma_{\text{smooth}} - \Sigma_{\text{original}}) / \Sigma_{\text{smooth}}$. With open diamonds we plot the median value of δ in each elliptical annulus, as a function of the semi-major axis: this quantity illustrates the balance between the number of pixels that are scattered above and below their original value. The solid lines represent the mean value of δ , which gives a measure of how well the SB is conserved. Black symbols and lines are used for the median smoothing mode, while the red ones are for the mean smoothing. As in Fig. 3, the three panels in each row are for no smoothing level cut, cut level 1, and the cut to exclude all but the levels above the current minus 2. The two rows show the results for the full image (bottom row) and for the image where masked regions have been excluded (top row). The main thing to note is that, with very few exceptions, all deviations are positive: the adaptively smoothed images have a bias to higher surface brightness with respect to the original. The reason for this bias is essential to the adaptive scheme: as the smoothing aperture is increased until the requested S/N is reached, the code tends to get rid of negative noise fluctuations by forcing a stronger smoothing, while positive fluctuations are not contrasted. This bias is of the order of 2% at most if the whole image is considered, 1% if we neglect the bright spots

(masked regions).

Let's now consider the smoothing modes without level cuts (panels in the first column of Fig. 4) in more detail. By using *median* smoothing, the median δ is 0 with only a few exceptions at large radii (i.e. low SB) and this indicates that the number of pixels with positive and negative variations almost balance, as expected for a symmetric noise distribution. However, the mean δ has most of the time positive values, as a consequence of the bias discussed before. It is noticeable that the masked regions have relatively little impact both on the median and on the mean bias, thus indicating the robustness of the median smoothing mode. On the contrary, the *mean*-smoothed images are generally more strongly biased toward higher SB, as shown by both median and mean δ profiles. Also, by comparing the top and bottom panels, and as already seen in the previous section, the mean smoothing is much more sensitive to and, hence, biased by, the presence of bright spots on top of low-SB regions.

The top row of Fig. 4 demonstrates that, once the problematic regions are taken out, the use of level cuts either in mean- or median-smoothing mode makes essentially no difference. The only notable exception is that cutting level 1 reduces the relative SB bias from 0.003 to < 0.001 in the region between 50 and 100 pixels, which corresponds to the transition from the high-SB where no smoothing is required to lower-SB. On the other hand, the bottom row of Fig. 4 demonstrates that on the full image (including the masked regions, which is the normal case in practice) the use of level cuts can significantly reduce the SB bias below 1% level in mean-smoothing mode, hence comparable to what one gets in median-smoothing mode.

In Fig. 5 we show how the smoothing performed with ADAPTSMOOTH affects two classical photometric measurements, that is azimuthally averaged SB profiles and growth curves of magnitude. In the left-hand panels we plot the difference in surface brightness between the azimuthally averaged profiles obtained on the ADAPTSMOOTH-ed images with different modes and parameters and the original image, both for the masked and the full images (upper and lower panels, respectively). These plots basically mirror the mean

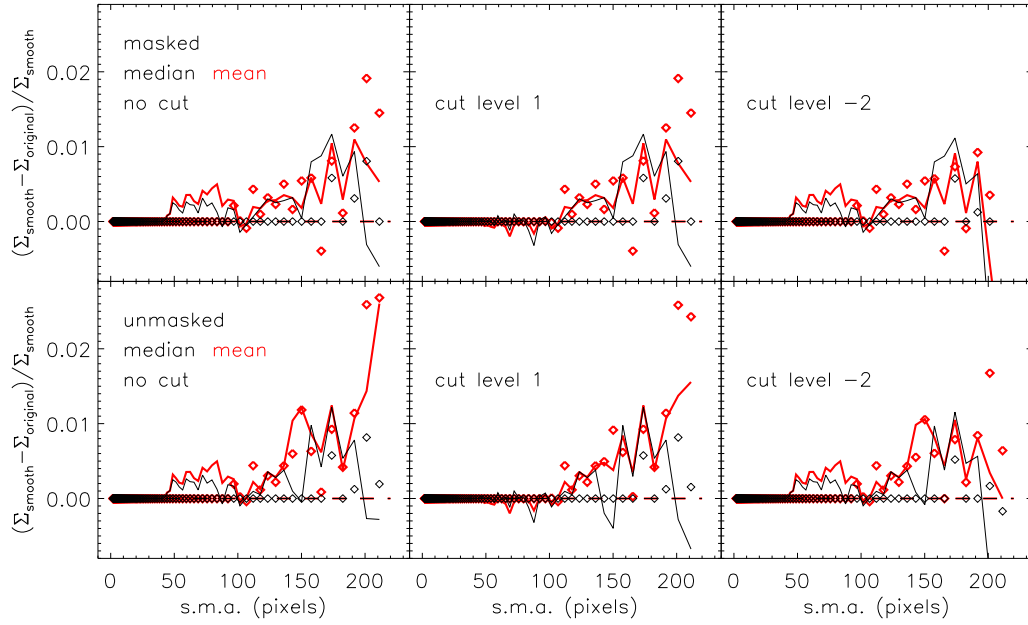


Figure 4: Statistics of relative difference of pixel brightness in NGC 5713 after and before ADAPTSMOOTH-ing, as a function of radius and for different modes and parameters (as indicated in the legends, black is for median-smoothing, red for mean-smoothing). Solid lines show the mean relative differences, while diamonds are median differences. The *bottom* row is relative to the full image, in the *top* row masked areas (see Fig. 2) are neglected.

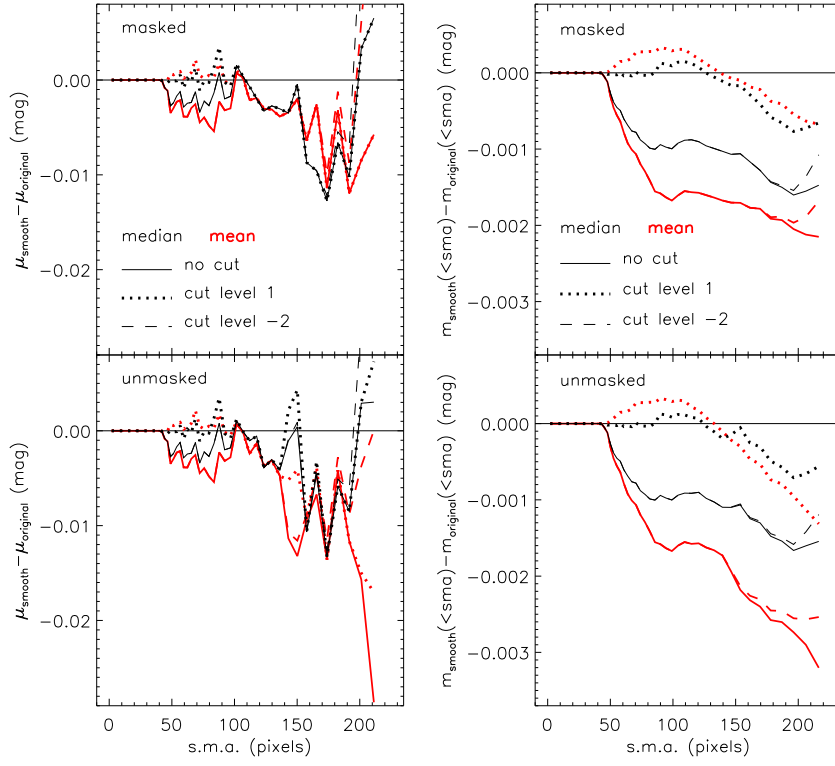


Figure 5: Deviations of the SB-profiles (*left* column) and of the growth curves (*right* column) of ADAPTSMOOTH-ed images of NGC 5713 with respect to the original. As indicated in the legends, black is for median-smoothing, red for mean-smoothing; different lines are used for different smoothing level cuts. The *bottom* plots refer to the full image, in the *top* plots masked areas (see Fig. 2) are neglected.

curves of Fig. 4 and show that the SB in smoothed images is biased brighter by no more than 0.01 mag approximately. The same remarks about smoothing modes and level cuts as made for Fig. 4 apply also here.

The growth curves (right-hand panels) show that flux is conserved in the smoothed images at better than 0.003 mag (0.002 mag when problematic regions are masked out). The regions that have the largest influence in biasing the total flux high are not the bright spots on top of low-SB regions, however, but those regions at the transition between no smoothing and smoothing level 2. Using median- instead of mean-smoothing already reduces this effect by $\approx 50\%$, although the best results are obtained by cutting level 1 in addition: in this case the flux is conserved with an accuracy of < 0.001 mag. Other level cuts that do not exclude level 1 have marginally influence on flux conservation.

As a general conclusion of this section on testing ADAPTSMOOTH on galaxy photometry, we can say that the best results in terms of minimizing artifacts, conserving surface brightness and total flux are obtained with median-smoothing mode and by cutting smoothing level 1. We remind the reader and the user that this configuration may not be ideal in all cases, depending on the typical contrast of the images to be processed and their photon statistics. A notable example is the case of extremely low photon-count rates, discussed at the end of Sec. 2.1, where mean-smoothing has definitely to be preferred to median-smoothing. ADAPTSMOOTH offers the user full flexibility and a full range of options (which are unavailable or only partly available in other public codes) which can be best adapted to different imaging datasets.

4 Summary

We have introduced ADAPTSMOOTH, a new standalone code to perform adaptive smoothing of astronomical images, which is made publicly available. ADAPTSMOOTH uses either median or arithmetic-mean average within apertures whose size is variable and determined in order to provide pixel sur-

face brightness measurements above the minimum requested S/N. In this way the best compromise between photometric accuracy and spatial resolution is obtained at any location of an image. The use of smoothing masks allows to work with multi-band imaging and hence to spatially resolve the spectral energy distribution of extended objects. Adaptive smoothing extends to much dimmer surface brightness the ability of measuring local fluxes and colours and hence can have a very strong impact on the study of extended objects, such as galaxies (as shown, e.g., in Zibetti et al. 2009, 2010) and nebulae (see Fig. 1).

We provide and discuss different ways to estimate local S/N in an image (based on Poisson+background noise, on background noise only, or on local signal fluctuations) and options to reduce artifacts (smoothing level cuts). Finally, we analyze in detail the qualitative and quantitative effects of adaptive smoothing on galaxy images. In the best operation mode for a typical optical image (i.e. median smoothing and smoothing level cut 1) the azimuthally averaged SB profile of the smoothed images deviates by less than 0.01 mag from that of the original image, while the flux growth curve deviates by less than 0.001 mag.

Compared to other existing codes for adaptive smoothing, ADAPTSMOOTH provides the broadest variety of options to operate in different regimes. In particular, ADAPTSMOOTH uniquely implements a median-averaging mode, which turns out to provide best results in terms of flux conservation and minimization of artifacts originating from bright sources when the photon statistics are well populated. The use of smoothing level cuts is much more flexible than in other codes (e.g. in CSMOOTH). Finally, the three possible choices for S/N estimate cover essentially all regimes for typical optical and near-IR images (as well as for shorter wavelengths) and guarantee good results even with minimal knowledge of the data error model. Such support is only partly provided by other adaptive smoothing codes (e.g. CSMOOTH supports Poisson and background dominated noise, but no direct r.m.s. estimate on the image, while XMM ASMOOTH only supports Poisson errors or user provided variance maps).

Acknowledgments

We thank Paolo Franzetti and Anna Gallazzi for useful comments and for helping in testing the code, and Arjan Bik for kindly providing the images of NGC2024.

References

- Bik, A., Lenorzer, A., Kaper, L., et al. 2003, *A&A*, 404, 249
- Blackburn, J. K. 1995, in *Astronomical Society of the Pacific Conference Series*, Vol. 77, *Astronomical Data Analysis Software and Systems IV*, ed. R. A. Shaw, H. E. Payne, & J. J. E. Hayes, 367–+
- Busko, I. C. 1996, in *Astronomical Society of the Pacific Conference Series*, Vol. 101, *Astronomical Data Analysis Software and Systems V*, ed. G. H. Jacoby & J. Barnes, 139–+
- Cappellari, M. & Copin, Y. 2003, *MNRAS*, 342, 345
- Ebeling, H., White, D. A., & Rangarajan, F. V. N. 2006, *MNRAS*, 368, 65
- Floyd, R. W. & Rivest, R. L. 1975, *Commun Acn*, 18, 173
- Huang, Z. & Sarazin, C. L. 1996, *ApJ*, 461, 622
- Jedrzejewski, R. I. 1987, *MNRAS*, 226, 747
- Martínez-Delgado, D., Gabany, R. J., Crawford, K., et al. 2010, *AJ*, 140, 962
- Mentuch, E., Abraham, R., & Zibetti, S. 2010, *ApJ*, 725, 1971
- Pasquali, A., Bik, A., Zibetti, S., et al. 2011, *AJ* in press, arXiv:1101.3221
- Pence, W. 1999, in *Astronomical Society of the Pacific Conference Series*, Vol. 172, *Astronomical Data Analysis Software and Systems VIII*, ed. D. M. Mehringer, R. L. Plante, & D. A. Roberts, 487–+
- Salim, S. & Rich, R. M. 2010, *ApJ*, 714, L290
- Sanders, J. S. 2006, *MNRAS*, 371, 829
- York, D. G. & et al. 2000, *AJ*, 120, 1579
- Zibetti, S., Charlot, S., & Rix, H. 2009, *MNRAS*, 400, 1181
- Zibetti, S., Charlot, S., & Rix, H. 2010, in *IAU Symposium*, Vol. 262, *IAU Symposium*, ed. G. Bruzual & S. Charlot, 89–92